ResearchGate

See discussions, stats, and author profiles for this publication at: https://www.researchgate.net/publication/221724016

Phosphorescent Organic Light-Emitting Diodes with Outstanding External Quantum Efficiency using Dinuclear Rhenium Complexes as Dopants

ARTICLE *in* ADVANCED MATERIALS · APRIL 2012

Impact Factor: 17.49 · DOI: 10.1002/adma.201104831 · Source: PubMed

CITATIONS
32

READS
49

7 AUTHORS, INCLUDING:

Cheng-Han Yang

39 PUBLICATIONS **1,431** CITATIONS

SEE PROFILE

Monica Panigati

University of Milan

37 PUBLICATIONS **481** CITATIONS

SEE PROFILE

Chih-Hao Chang

Yuan Ze University

69 PUBLICATIONS **1,728** CITATIONS

SEE PROFILE

Giuseppe D'Alfonso

University of Milan

97 PUBLICATIONS **1,557** CITATIONS

SEE PROFILE

Available from: Chih-Hao Chang
Retrieved on: 15 January 2016

COMMUNICATION

Phosphorescent Organic Light-Emitting Diodes with Outstanding External Quantum Efficiency using Dinuclear Rhenium Complexes as Dopants

Matteo Mauro, Cheng-Han Yang, Chin-Yao Shin, Monica Panigati, Chih-Hao Chang,* Giuseppe D'Alfonso, and Luisa De Cola**

Nowadays, organic light-emitting diodes (OLEDs) are becoming a more and more fascinating field in both fundamental and applied research, due to their potential application in flat panel display and lighting technology.[1] It has been shown that OLED-based technology can possess superior characteristics with respect to the purely inorganic semiconductor-based LED, such as flexibility, color rendering, higher efficiency and low operating voltage as well as low cost fabrication. More recently, in order to enhance the performances of OLED devices, electrophosphorescent materials incorporating organometallic compounds have been employed. OLEDs using luminescent heavy metal complexes (PhOLEDs) are able to harvest both singlet and triplet electro-generated excitons, thus rising the theoretical quantum efficiency from 25% to 100%, when compared with devices based on purely fluorescent materials.[2] Indeed, luminescent transition metal complexes can show emission from the lowest-lying triplet-manifold long-lived excited state, whose characteristics can be modulated by proper choice of the metal and careful design of the ligands. In this respect, leading position is held by complexes based on iridium(III)[3] and platinum(II),[4] due to their outstanding photophysical properties, as wide color tunability, high photoluminescence quantum yields (PLQYs)[5] and often reversible electrochemical characteristics.

To the best of our knowledge, phosphorescent OLEDs showing maximum external quantum efficiency (EQE) of 29.6%,[6] and 11.5%,[7] when doped with iridium- and platinum-based complexes, respectively, have been very recently reported. Furthermore, PhOLEDs doped with tri-coordinated complexes based on the more abundant and cheaper copper(I) have shown maximum EQE as high as 21.3%.[8] On the other hand, only marginal contributions in terms of efficiency enhancement have been displayed by other classes of complexes, mainly based on ruthenium(II),[9] osmium(II),[10] and rhenium(I),[11] because of their generally less performing properties. Nevertheless, the possibility for OLED devices, with performances high enough to become appealing for being a real market technology, strongly implies the constant pursuit of new and more efficient materials, with reduced nonradiative quenching processes also at higher concentrations.[12]

We report on interesting photo- and electro-luminescence properties of two highly emissive dinuclear rhenium carbonyl complexes, which belong to the novel class recently described by our group.[11a,13] As demonstrated below, the efficient use of these complexes as emitting material in vacuum-processed PhOLEDs gives devices with maximum EQE of ca. 10%. These values are the highest ever reported for PhOLEDs with rhenium-based phosphors, undoubtedly comparable with state-of-the-art devices employing platinum-based triplet emitters, and approaching efficiencies of iridium-based dopants.

The dinuclear rhenium carbonyl complexes here investigated are depicted in **Figure 1** and have general formula [Re_2(μ-halogen)$_2$(CO)$_6$(μ-1,2-diazine)], where halogen and 1,2-diazine are Cl and 6,7-dihydro-5*H*-cyclopentapyridazine, for **1**, and Br and pyridazine, for **2**, respectively. Their synthesis and photophysical characterization in solution were previously described by our group.[11a,13] At room temperature in degassed fluid toluene solution and upon optical excitation in the range 300–400 nm, both complexes displayed a broad and featureless emission, attributed to a transition from lowest-lying triplet-manifold excited state ($T_1 \rightarrow S_0$) with metal-to-ligand charge transfer (^{3}MLCT) nature, centered at 547 and 620 nm for **1** and **2**, respectively. Noteworthy, whilst **1** showed excited-state lifetime of 5.3 μs and PLQY of 53%, **2** displayed a strongly quenched emission, with lifetime of 20 ns and PLQY of only 0.2%. This has been attributed[13] to the bulkiness of the Br atoms in complex **2**, which imposes a Re–Re distance much longer than the optimum for bridging coordination of the diazine. As a consequence, a distorted and floppy coordination sphere with possible reversible bridge opening and fast interchange between bridging and terminal coordination resulted.

We have now found an interesting behavior in solid state for these two complexes with very similar chemical structure. Both derivatives display ipsochromically-shifted emission in

Dr. M. Mauro, Dr. C.-H. Yang, Prof. L. De Cola
Physicaliches Institut and Center for Nanotechnology (CeNTech)
Westfälische Wilhelms Universität Münster
Mendelstrasse, 7 48149 Münster, Germany
E-mail: matteo.mauro@uni-muenster.de; decola@uni-muenster.de
C.-Y. Shin, Prof. C.-H. Chang
Department of Photonics Engineering
Yuan Ze University
Chungli, 32033, Taiwan
E-mail: chc@saturn.yzu.edu.tw
Dr. M. Panigati, Prof. G. D'Alfonso,
Dipartimento di Chimica Inorganica
Metallorganica ed Analitica "Lamberto Malatesta"
Università degli Studi di Milano
and UdR INSTM of Milano
Via Venezian 21, 20133 Milano, Italy

DOI: 10.1002/adma.201104831

© 2012 WILEY-VCH Verlag GmbH & Co. KGaA, Weinheim

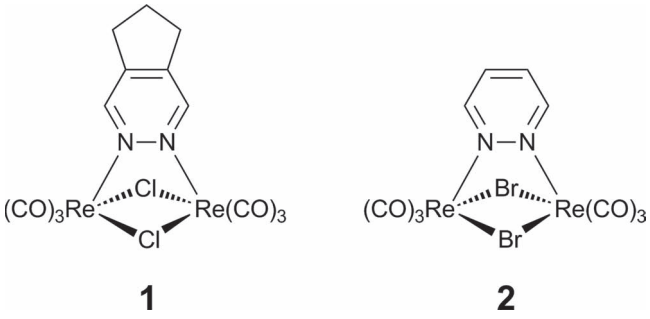

Figure 1. Chemical formulas of the complexes **1** and **2**.

neat-powder with respect to the diluted solution (493 vs. 547 and 560 vs. 620 nm, for **1** and **2**, respectively), in agreement with the rigidochromic effect usually observed for charge transfer emission.[14] Nonetheless, as neat powder sample, while the emission efficiency of complex **1** is significantly weaker, dropping from 53% to 10%, complex **2** displays enhanced and much brighter luminescence (PLQY increasing from 0.2% to 49%), with bi-exponential lifetime decay of few μs. Similarly, in poly(methyl methacrylate) (PMMA) thin-film, whilst for the highly emitting in solution complex **1**, the PLQY dropped again down to 10–11%, independently of the concentration, complex **2** displayed a noticeable enhancement of the PLQY with values as high as 11–27%, depending on the concentration. In particular, at 2 wt% doping concentration, complex **2** still displays brighter emission than **1** (λ_{em} = 556 nm, PLQY 27% for **2** vs. λ_{em} = 527 nm, PLQY 11% for **1**). In the Supporting Information (SI), Figures S1–S3 show the emission profiles in thin-film made using PMMA and different concentration of **1** and **2**. In SI, Table S1 summarizes the most meaningful photophysical data.

The emission enhancement for **2** is accompanied by a strong decrease of the radiationless rate constant (k_{nr}) which drops from 4.99×10^7 to $2.39–5.03 \times 10^5$ s^{-1}, going from solution to solid state, whilst the radiative rate constant (k_r) remains on the same order of magnitude (1.30×10^5 vs. $0.49–2.30 \times 10^5$ s^{-1}). These data agree with the idea that the emission of **2** in solution is almost completely quenched by the above mentioned lability of the $Re_2(\mu\text{-}Br)_2(\mu\text{-diazine})$ core, and it is restored in solid, due to the lower mobility imposed by the more rigid environment. The fact that as solid powder complex **2** shows such a bright emission can be identified as an example of aggregation-induced emission (AIE),[12b,15] a phenomenon which has been already deeply investigated by our group for another component of this class of dinuclear Re(I) emitters.[16] Noteworthy, in the present case the increase of PLQY from solution to solid state (more than two orders of magnitude) is even stronger than in the previously studied dirhenium-diazine complex (ca. 10 times),[16a] where the enhancement was attributed to the freezing of the intramolecular rotation of the Me_3Si substituents on the diazine ligand. For complex **2**, as mentioned above, the presence of the bridging Br plays an important role in the distortion of the structure, as also seen by the increased Re–Br–Re distance in the X-ray analysis compared with the shorter Re–Cl–Re distances.[16b] On the other hand, the larger polarizability of the Br vs. Cl and its good charge transport properties results in interesting emerging properties when **2** is used as dopant in electroluminescent devices. It is worth to note that the choice of these two complexes has been dictated by the fact that the analogous complex with pyridazine ligand and chloro-bridging atoms, namely $[Re_2(\mu\text{-}Cl)_2(CO)_6(\mu\text{-pyridazine})]$, has shown to possess emission quantum yield of 5% in solution,[13] and of only 9% in solid state. Thus, complex **2** is a much better performing emitter than the analogous chloro-bridged compound. On such basis, we have selected complex **2** and the best emitter in solution (**1**).

We therefore decided to take advantage of the behaviour in solid matrices of the complexes and to test them in electroluminescent devices obtained by using the two compounds as dopants in vacuum-processed PhOLEDs. Even though the use of **1** as dopant in devices has been already reported by our group,[11a] it has been here investigated for a proper comparison with **2**, being now employed in identical device architectures. The results show that there is indeed an important role played by the different chemical structures and we have reached excellent external efficiencies, even though we have used a very simple device architecture.

It is worth noticing in fact that the preparation of multi-layer OLED architectures is exceedingly cumbersome and complicated, making mass production fraught with difficulties and usually low yield fabrication. Therefore, a simple three-organic layers configuration, namely hole-transporting (HTL), emitting-(EML) and electron-transporting (ETL) layers, was chosen in this study.

In a first set of devices different hole and electron transporting layers have been tested. The wide triplet-gap materials 4,4′-*N*,*N*′-dicarbazole-biphenyl (CBP) and di-[4-(N,N-ditolyl-amino)-phenyl]cyclohexane (TAPC), were selected as host and HTL,[17,18] respectively, for ensuring efficient exothermic energy transfer and exciton confinement, and complex **2** as dopant. In order to optimize device performances and obtain the best carrier balancing condition upon device operation, ETL, and doping concentration were varied. In particular, the following electron transporting materials were investigated: 3-(4-biphenylyl)-4-phenyl-5-(tert-butylphenyl)-1,2,4-triazole (TAZ), 1,3,5-tri[(3-pyridyl)-phen-3-yl]benzene (TmPyPB), 2,2′,2″-(1,3,5-benzinetriyl)-tris(1-phenyl-1-H-benzimidazole) (TPBi), and 3,5,3′,5′-tetra(m-pyrid-3-yl)phenyl[1,1′]biphenyl (BP4mPy).[19,20] The chemical structure of the materials is depicted in SI, Figure S4. The simplified architecture of the devices can be described as follows: ITO/TAPC (40 nm)/CBP doped with 8 wt% of **2** (30 nm)/ETL (40 nm)/LiF (0.8 nm)/Al (150 nm).

Better EQEs were generally obtained for the device employing whether TmPyPB or BP4mPy. However, for the former at higher luminance the electroluminescence (EL) spectra showed an unwanted near-UV emission and a red-shift of the emission of the dopant. Such results are shown in Figure S5 and Table S2 of the Supporting Information. Moreover, the corresponding current density–voltage–luminance (*J*–*V*–*L*) curves indicated a much higher turn-on voltage (data not shown). Hence, upon typical doping concentration of 8 wt% for the Re(I)-based triplet emitter (complex **2**) the best performances were obtained when BP4mPy was used as ETL, mainly due to its adequate mobility and wide triplet-energy gap. On the other hand, devices using electron transporting materials with lower-gaps or inadequate

© 2012 WILEY-VCH Verlag GmbH & Co. KGaA, Weinheim

Table 1. Electroluminescence characteristics for the devices with the following architecture: ITO/TAPC (40 nm)/mCP: dopant **x** wt% (30 nm)/BP4mPy (40 nm)/LiF (0.8 nm)/Al (150 nm).

dopant		EQE [%]		LE [cd A^{-1}]		PE [lm W^{-1}]		turn-on voltage[a)] [V]	max. brightness [cd m^{-2}]	CIE coordinates	
		max.	@ 10^2 cd m^{-2}	max.	@ 10^2 cd m^{-2}	max.	@ 10^2 cd m^{-2}			@ 10^2 cd m^{-2}	@ 10^3 cd m^{-2}
1	1 wt%	5.2	4.4	14.8	12.4	11.0	6.0	4.2	3077 (14.0 V)	(0.303, 0.516)	(0.282, 0.464)
	2 wt%	5.9	5.2	17.9	15.8	12.6	8.5	4.1	2306 (13.2 V)	(0.310, 0.536)	(0.294, 0.509)
2	1 wt%	10.0	9.7	30.3	29.6	22.6	16.3	3.9	5032 (13.4 V)	(0.425, 0.543)	(0.421, 0.535)
	2 wt%	9.8	9.5	29.2	28.5	22.1	15.8	3.9	9921 (14.0 V)	(0.438, 0.536)	(0.436, 0.535)

[a)]The turn-on voltage refers to the voltage at which the brightness reaches the value of 1 cd m^{-2}.

electron-mobility capabilities, such as TAZ and TPBi, showed inferior performances.

On the basis of the above described results, a new set of devices was made, in which the dopant concentration varied in the range 1–8 wt% and selecting BP4mPy as ETL, TAPC as HTL, and CBP as matrix. The EL performance data of devices with different concentration are depicted in SI, Figures S6–S7 and Table S3. At concentration as low as 1 wt% in CBP, the EL spectra showed remarkable near-UV emission, attributable to the BP4mPy layer,[20] whose relative intensity increased upon increasing the operation driving voltages.

This near-UV emission obviously dropped when the doping concentration exceeded 2 wt%, which represented the minimum request for an efficient energy transfer process between the host material and the dopant. It is worth noticing that these lower band-gap rhenium complexes also play a role as effective carrier-trapping material in the CBP host. Indeed, going from 1 to 2 wt% in concentration of phosphorescent dopant will promote charge recombination in the EML, thus drastically reducing the probability of exciton formation in the ETL.

Devices with concentration higher than 2 wt% exhibited slightly inferior performances (see SI, Figure S7). Nevertheless, at higher current densities the efficiency curves of all the devices were almost the same, whichever the dopant concentration, implying that the latter parameter has limited impact on the efficiency roll-off. On the basis of the results of EL spectra and efficiencies of the tested devices, the optimum concentration was set to 2 wt% for complex **2**.

In order to ensure even better exciton confinement in the EML for both dopants, a different host material, namely 3-bis(9-carbazolyl)benzene (mCP),[21] was now used to build up the devices and the rhenium-complex concentration varied in the range 1–2 wt% (see **Table 1**). For both complexes, the devices with different concentrations gave similar efficiency performances, and those at 2 wt% will be hereafter referred to as device A, for complex **1**, and B, for complex **2**. For the selected materials, the chemical structure and the pictorial energy-level diagram are depicted in **Figure 2**. The electroluminescence (EL) characteristics are shown in **Figure 3**.

In this configuration the sharp energy-barriers (>0.6 eV) at both the TAPC/mCP and mCP/BP4mPy interfaces (Figure 2) should effectively suppress the draining of charge carriers from the EML to the nearby charge transporting layers, i.e., TAPC and BP4mPy, thus acting also as electron- (EBL) and hole-blocking (HBL) layers, respectively. However, mCP possesses noticeable hole transporting capability, and then the exciton formation zone is mainly located near the mCP/BP4mPy interface. Hence, the unwanted near-UV emission should be the result of a high-energy exciton migration from the formation zone, i.e., the mCP host, towards the BP4mPy layer.

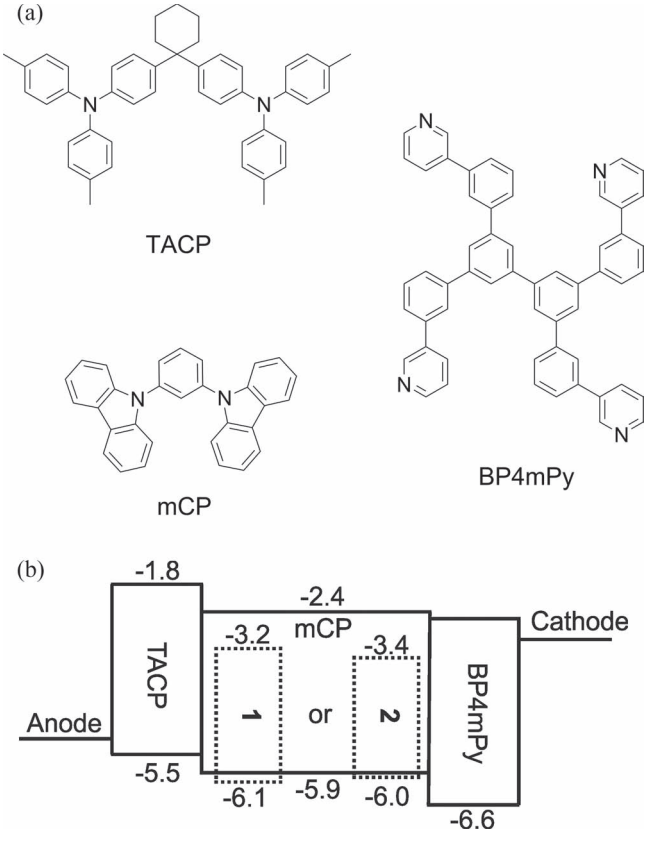

Figure 2. a) chemical formulas of materials used in the OLED devices A and B; b) simplified energy-level diagram of the different layers and electrodes in the devices.

Both devices predominantly displayed the typical emission of the corresponding triplet emitting dopant in PMMA thin-film.

© 2012 WILEY-VCH Verlag GmbH & Co. KGaA, Weinheim

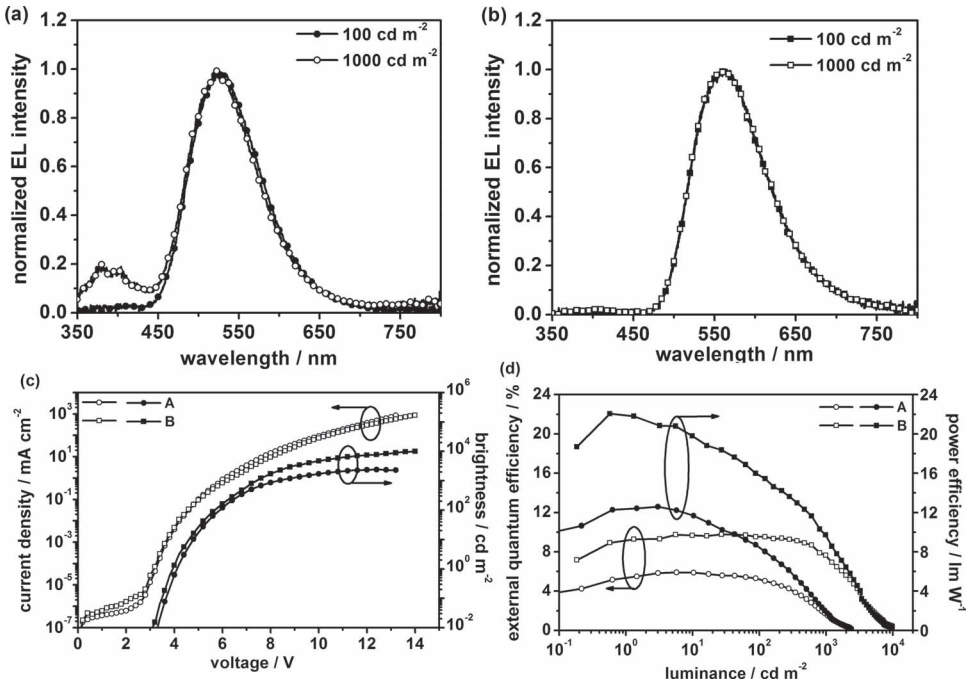

Figure 3. Electroluminescence characteristics of the devices incorporating complexes **1** and **2** as dopant, with the following architecture: ITO/TAPC (40 nm)/mCP:Re complex (2 wt%) (30 nm)/BP4mPy (40 nm)/LiF (0.8 nm)/Al (150 nm): a) EL spectrum of the device A; b) EL spectrum of the device B; c) current density–voltage–luminance (*J–V–L*) *characteristics* plots; d) external quantum efficiency (EQE) and power efficiency (PE) vs. luminance plots.

However, in the case of device A, when driven at high current densities, the greenish-yellow emission of complex **1** (λ_{EL} = 527 nm) was still accompanied by a residual weak emission attributable to BP4mPy (λ_{EL} = 380 and 402 nm) (Figure 3a). The latter emission was much mitigated in device B (Figure 3b), whose yellow emission (λ_{EL} = 565 nm) arises exclusively from complex **2** even at high current densities, indicating that in this device the exciton formation zone is located further away from the mCP/BP4mPy interface. On the basis of such findings, it is possible to argue a better electron transporting capability for complex **2** with respect to **1**. Noteworthy, the emission colors from device B were extremely stable over a wide luminance range, with CIE(*x*,*y*) emission color coordinates of 0.44, 0.54 (see Table 1).

In Figure 3c,d the current density–voltage–luminance (*J–V–L*) and efficiencies curves for both devices are depicted, respectively. As far as the efficiencies are concerned in the applied forward bias, device A exhibited a peak photon-to-electron efficiency of 5.9%, luminance efficiency (LE) of 17.9 cd A^{-1}, and power efficiency (PE) of 12.6 lm W^{-1}. Moreover, at the practical brightness of 100 cd m^{-2} the efficiencies remained still high, with maximum EQE of 5.2%, LE of 15.8 cd A^{-1}, and PE of 8.5 lm W^{-1} (see also Table 1). These performances overcame the previously reported device using complex **1** as emitting dopant.[11a] Even more interestingly, device B exhibited a lower turn-on voltage (3.9 V), and a remarkable maximum EQE of 9.8% (at 5.0 V), peak LE of 29.2 cd A^{-1}, and PE of 22.1 lm W^{-1}. Moreover, it displayed much better efficiency at higher current densities with respect to that fabricated using complex **1**, and remarkably, the efficiencies remained still noticeably high at the practical brightness of 100 cd m^{-2}, being 9.5%, 28.5 lm W^{-1} and 15.8 cd A^{-1}, respectively (Table 1). Comparing the efficiency roll-off behavior of both devices, the EQEs of the here reported PhOLEDs decreased to half at a current density ($J_{1/2}$) of 6.52 mA cm^{-2} and 17.2 mA cm^{-2}, for device A and device B, respectively.[22] In general, both triplet–triplet annihilation (TTA) and triplet–polaron quenching are commonly observed under typical PhOLED operations and TTA is pointed as the main mechanism for efficiency decrease at higher luminance regimes.[23] Such mitigated efficiency roll-off shown by device B with respect to device A once again might indicate that the exciton formation is not localized at the mCP/BP4mPy interface. On the contrary, the exciton formation layer is now spread all over the EML, confirming the aforementioned better electron-transporting capability of complex **2**.

In conclusion, we have shown that complex **2** provides an impressive example of enhancement of the emission efficiency upon rigidification of the matrix and as pure solid a remarkable aggregation induced luminescence, featuring in solid greenish-yellow emission, with PLQY of 49% (vs. 0.2% in solution) with relatively short triplet-manifold excited-state lifetime (few μs). Its structure comprising a dinuclear system bridged by Br units is important for its charge transporting properties. Such features helped **2** to be successfully employed as emitting dopant in the fabrication of vacuum-processed PhOLEDs, which, in this preliminary study, reached remarkable peak EQE as high as 9.8%, LE of 29.2 cd A^{-1}, and PE of 22.1 lm W^{-1}, despite of the simple device architecture used. Even though complex **2** was orders of magnitude less emissive than complex **1** in dilute solution, an efficiency improvement of about 1.7 times, with respect to

© 2012 WILEY-VCH Verlag GmbH & Co. KGaA, Weinheim

1, has been obtained by employing **2** as triplet emitter, in the same device architecture. Furthermore, the noticeable decrease of the near-UV emission from the ETL, observed even at high current densities in the device doped with **2**, suggested a higher electron transporting capability of **2**, which strongly contributed to properly locate the exciton recombination zone into the EML. These encouraging results demonstrated that the development of new highly solid-state emitting dinuclear rhenium(I) complexes for efficiently performing PhOLEDs possesses promising potential as alternative to the iridium- and platinum-based triplet emitters.

Experimental Section

General Methods: The energy values of the reported HOMO and LUMO levels are measured by means of cyclic voltammetry,[11a,13] and referred to the vacuum level by using the following empirical relation: $E^{HOMO,LUMO} = -eE^{ox,red} - 4.8$ eV, where $E^{HOMO,LUMO}$ is the energy level of the HOMO (LUMO), and $E^{ox,red}$ are the electrochemical oxidation (reduction) potentials of the molecule measured in solution, referred to $Fc^+|Fc$ couple, respectively.[24]

Photophysical Characterization: Steady-state and time-resolved luminescence experiments, as well as absolute quantum yield determination were carried out by using experimental setups already reported.[11a]

OLED Preparation and Characterization: The materials used were purchased from Nichem and purified by temperature-gradient sublimation under high vacuum before use. Substrates were previously cleaned by exposure for 5 min to a UV–ozone atmosphere. OLED devices were fabricated using indium tin oxide (ITO) coated glass substrates (<15 Ω) with multiple organic layers, sandwiched between the transparent bottom ITO anode and the top metal cathode. The organic and metal layers were deposited by thermal evaporation in a vacuum chamber with a base pressure $<10^{-6}$ torr without breaking the vacuum. Deposition rate of the organic layers was kept at around 0.1 nm s^{-1}. The active area of the device was 2×2 mm^2, as defined by the shadow mask used for cathode deposition. Current–voltage–luminance characterization was performed using an Agilent4156C semiconductor parameter analyzer equipped with a calibrated Si-photodiode. Electroluminescence spectra of the devices were recorded by using an Ocean Optics spectrometer.

Supporting Information

Supporting Information is available from the Wiley Online Library or from the author.

Acknowledgements

MM gratefully thanks the Alexander von Humboldt Foundation for financial support. CHC and CYS gratefully acknowledge the financial support from the National Science Council of Taiwan (NSC 99-2221-E-155-035-MY3) and the Ministry of Economic Affairs (100-EC-17-A-08-S1-042).

Received: December 18, 2011
Published online: March 19, 2012

[1] B. D'Andrade, *Nat. Photon.* **2007**, *1*, 33.
[2] a) *Highly Efficient OLEDs with Phosphorescent Materials* (Ed: H. Yersin) Wiley-VCH, Weinheim, Germany **2008**; b) M. E. Thompson, P. E. Djurovich, S. Barlow, S. Marder in *Comprehensive Organometallic Chemistry III* (Ed: R. H. Crabtree, D. M. P. Mingos), Elsevier, Oxford, UK **2006**.
[3] a) S.-C. Lo, R. E. Harding, C. P. Shipley, S. G. Stevenson, P. L. Burn, I. D. W. Samuel, *J. Am. Chem. Soc.* **2009**, *131*, 16681; b) C.-H. Yang, Y.-M. Cheng, Y. Chi, C.-J. Hsu, F.-C. Fang, K.-T. Wong, P.-T. Chou, C.-H. Chang, M.-H. Tsai, C.-C. Wu, *Angew. Chem. Int. Ed.* **2007**, *46*, 2418; c) S. Lamansky, P. Djurovich, D. Murphy, F. Adbel-Razzaq, H.-E. Lee, C. Adachi, P. E. Burrows, S. R. Forrest, M. E. Thompson, *J. Am. Chem. Soc.* **2001**, *123*, 4304.
[4] a) C. A. Strassert, C.-H. Chien, M. D. Galvez Lopez, D. Kourkoulos, D. Hertel, K. Meerholz, L. De Cola, *Angew. Chem. Int. Ed.* **2011**, *50*, 946; b) J. Kalinowski, V. Fattori, M. Cocchi, J. A. G. Williams, *Coord. Chem. Rev.* doi:10.1016/j.ccr.2011.01.049.
[5] a) T. Sajoto, P. Djurovich, A. B. Tamayo, J. Oxgaard, W. A. Goddard III, M. E. Thompson, *J. Am. Chem. Soc.* **2009**, *131*, 9813; b) Y. Kawamura, K. Goushi, J. Brooks, J. J. Brown, H. Sasabe, C. Adachi, *Appl. Phys. Lett.* **2005**, *86*, 71104.
[6] R. Wang, D. Liu, H. Ren, T. Zhang, X. Wang, J. Li, *J. Mater. Chem.* **2011**, DOI: 10.1039/c1jm10757g.
[7] A. Y.-Y. Tam, D. P.-K. Tsang, M.-Y. Chan, N. Zhu, V. W.-W. Yam, *Chem. Commun.* **2011**, *47*, 3383.
[8] M. Hashimoto, S. Igawa, M. Yashima, I. Kawata, M. Hoshino, M. Osawa, *J. Am. Chem. Soc.* **2011**, *133*, 10348.
[9] Y.-L. Tung, L.-S. Chen, Y. Chi, P.-T. Chou Y.-M. Cheng, E. Y. Li, G.-H. Lee, C.-F. Shu, F.-I. Wu, A. J. Carty, *Adv. Funct. Mater.* **2006**, *16*, 1615.
[10] T.-C. Lee, J.-Y. Hung, Y. Chi, Y.-M. Cheng, G.-H. Lee, P.-T. Chou, C.-C. Chen, C.-H. Chang, C.-C. Wu, *Adv. Funct. Mater.* **2009**, *19*, 2639.
[11] a) M. Mauro, E. Quartapelle Procopio, Y. Sun, C.-H. Chien, D. Donghi, M. Panigati, P. Mercandelli, P. Mussini, G. D'Alfonso, L. De Cola, *Adv. Funct. Mater.* **2009**, *19*, 2607; b) X. Li, D. Zhang, W. Li, B. Chu, L. Han, J. Zhu, Z. Su, D. Bi, D. Wang, D. Yang, Y. Chen, *Appl. Phys. Lett.* **2008**, *92*, 083302.
[12] a) Y.-C. Zhu, L. Zhou, H.-Y. Li, Q.-L. Xu, M.-Y. Teng, Y.-X. Zheng, J.-L. Zuo, H.-J. Zhang, X.-Z. You, *Adv. Mater.* **2011**, *23*, 4041; b) W. Z. Yuan, S. Chen, J. W. Y. Lam, C. Deng, P. Lu, H. H-Y. Sung, I. D. Williams, H. S. Kwok, Y. Zhang, B. Z. Tang, *Chem. Commun.* **2011**, DOI: 10.1039/c1cc14122h.
[13] D. Donghi, G. D'Alfonso, M. Mauro, M. Panigati, P. Mercandelli, A. Sironi, P. Mussini, L. D'Alfonso, *Inorg. Chem.* **2008**, *47*, 4243.
[14] M. Wrighton, D. L. Morse, *J. Am. Chem. Soc.* **1974**, *20*, 998.
[15] Y. Hong, J. W. Y. Lam, B. Z. Tang, *Chem. Soc. Rev.* **2011**, DOI: 10.1039/c1cs15113d.
[16] a) E. Quartapelle Procopio, M. Mauro, M. Panigati, D. Donghi, P. Mercandelli, A. Sironi, G. D'Alfonso, L. De Cola, *J. Am. Chem. Soc.* **2010**, *132*, 14397; b) Unpublished single-crystal X-ray structures. For the corresponding DFT calculations please refer to ref. 13.
[17] a) B. E. Koene, D. E. Loy, M. E. Thompson, *Chem. Mater.* **1998**, *10*, 2235; b) D. F. O'Brien, M. A. Baldo, M. E. Thompson, S. R. Forrest, *Appl. Phys. Lett.* **1999**, *74*, 442.
[18] Y. Zheng, S.-H. Eom, N. Chopra, J. Lee, F. So, J. Xue, *Appl. Phys. Lett.* **2008**, *92*, 223301.
[19] a) K. Chen, C.-H. Yang, Y. Chi, C.-H. Chang, C.-C. Chen, C.-C. Wu, M.-W. Chung, Y.-M. Cheng, G.-H. Lee, P.-T. Chou, *Chem. Eur. J.* **2010**, *16*, 4315; b) P. Kundu, K. R. J. Thomas, J. T. Lin, Y.-T. Tao, C.-H. Chien, *Adv. Funct. Mater.* **2003**, *6*, 445; c) S.-J. Su, T. Chiba, T. Takeda, J. Kido, *Adv.Mater.* **2008**, *20*, 2125.
[20] S.-J. Su, D. Tanaka, Y.-J. Li, H. Sasabe, T. Takeda, J. Kido, *Org. Lett.* **2008**, *10*, 941.
[21] R. J. Holmes, S. R. Forrest, Y.-J. Tung, R. C. Kwong, J. J. Brown, S. Garon, M. E. Thompson, *Appl. Phys. Lett.* **2003**, *82*, 2422.
[22] S.-J. Su, E. Gonmori, H. Sasabe, J. Kido, *Adv. Mater.* **2008**, *20*, 4189.
[23] a) M. A. Baldo, S. R. Forrest, *Phys. Rev. B* **2000**, *62*, 10967; b) D. Hertel, K. Meerholz, *J. Phys. Chem. B* **2007**, *111*, 12075; c) S. Reineke, K. Walzer, K. Leo, *Phys. Rev. B* **2007**, *75*, 125328.
[24] S. Trasatti, *Pure Appl. Chem.* **1986**, *58*, 955.

© 2012 WILEY-VCH Verlag GmbH & Co. KGaA, Weinheim